9th ANKARA INTERNATIONAL AEROSPACE CONFERENCE **AIAC-2017-130**
20-22 September 2017 - METU, Ankara TURKEY

CONCEPTUAL DESIGN OF A LOW-BYPASS TURBOFAN ENGINE FOR NEXT GENERATION JET TRAINER

Olcay Sari* and Onur Tuncer†
Istanbul Technical University
Istanbul, Turkey

Orcun Bulat‡
Sapienza University of Rome
Rome, Italy

ABSTRACT

The paper presents conceptual design of a brand new low-bypass twin-spool turbofan engine with afterburner to replace J85-5A turbojet engine for new generation T-38 supersonic jet trainer aircraft. Starting with market evaluation of 5th generation fighter aircrafts and competitor jet trainers, constraint and mission analyses are made for preliminary estimations. With in-house developed parametric and performance analyses program, on and off design behaviors of potential twin-spool turbofan engines with afterburner are deeply examined. By the chosen design values, new engine components are developed. Composed by brand new 2-D 2-ramp inlet, counter rotating compressor stages, annular main combustor, CMC-based turbine stages, mixer, after-burner and convergent-divergent vectoring nozzle, new engine design is finalized. At the end, weight and cost estimations are performed. To summarize, the proposed design provides optimized cruise condition behavior, enhanced maximum speed capability, increased efficiency and performance characteristics, as well as extended range of 3333.6 km (1800 nmi).

INTRODUCTION

Nowadays in the jet engine industry, main challenges can be summarized as increasing Mach number capability while improving fuel consumption, providing high performance with weight reduction, range limitations and low operation & maintenance costs. In this study, conceptual design of a new turbofan engine that is solicited for an advanced trainer that is capable of replacing the T-38, which is expected to enter service around 2025 is made. New trainer has a plan form which is similar in wing and tail shape and arrangement to the T38A trainer, which will have supersonic dash over land and can also cruise at Mach 0.85, offering a lower cost-per-mile than the current version of T-38. Therefore, new engine must simulate 5th generation fighter aircraft missions and train pilots.

This design task is initiated according to the American Institute of Aeronautics and Astronautics (AIAA) Undergraduate Team Engine Design Competition 2016 request for proposal (RFP). The specific information about baseline engine is shown in table 1.

In design methodology, both educational materials and military reports are used. In-house codes are

*Graduate Student, Email: sariol@itu.edu.tr
†Assoc. Prof. in Aeronautics Department, Email: tuncero@itu.edu.tr
‡Graduate Student, Email: orcunbulat@gmail.com

Table 1: Baseline Engine: Basic Data, Overall Geometry and Performance

Design Features of the Baseline Engine	
Engine type	Axial, turbojet
Number of compressor stages	9
Number of HP turbines stages	2
Combustor type	Annular
Maximum net thrust at sea level (wet)	17.125 kN
Specific Fuel Consumption at max. power (wet)	224 kg/h/kN
Overall pressure ratio at max. power	6.7
Max. envelope diameter	44.96 cm
Max. envelope length	1.30 m
Dry weight less tailpipe	190.96 kg

developed to optimize the conditions by design parameters and to plot required graphs.

TECHNOLOGICAL STANDPOINT

At the beginning of the design phase, it is very important to be aware of the market situation of the industry to be working upon. For this reason, a wide range of research has been made for gathering information of jet trainer aircrafts and 5th generation fighters. Furthermore, their properties are very important for the new engine and its design due to the purpose of new trainer aircraft.

With the creation of 4th and 5th generation fighter aircrafts which are capable of high maneuvers and own enhanced avionic systems, new type of trainers – Advanced Jet Trainers have been developed to train latest generation pilots. While providing the opportunity of simulating latest fighter aircrafts missions and properties, the unit price and operational costs of the trainers should be as low as possible to fulfil their purpose, which is aimed for the next generation of T-38.

Table 2: Similar Supersonic Jet Trainer Aircraft Engines Specifications

	T-38 Talon		T-50 GE		Hongdu L-15		JL-9		F-5B	
Engine Type	J85-GE-5A		GE F404		AI-222-25F		Tumansky R-13		J85-GE-13	
Properties	DRY	WET	DRY	WET	DRY	WET	DRY	WET	DRY	WET
Thrust (kN)	11.9	17.1	48.9	78.7	24.7	41.2	39.9	63.7	12.1	18.2
TSFC (kg/h/kN)	105.06	224.4	82.62	177.48	67.32	193.8	82.82	213.18	128.52	226.44
Airflow (kg/s)	20		66.22		22.54		66		19.96	
OPR	6.7		26		15.43		8.9		6.5	
Bypass Ratio	-		0.34		1.19		N/A		-	
Compressors	9		3F, 0L, 7H		2L, 8H		3L, 5H		9	
Turbines	2		1H, 1L		1H, 1L		1H, 1L		2	
Diameter (cm)	55.8		88.90		62.38		109.47		55.88	
Length (m)	2.75		3.91		3.14		4.61		2.77	
Weight (kg)	264.90		1035.10		539.77		1204.74		270.79	

The latest generation of jet fighters – 5th encompasses the most advanced fighter aircrafts. Even though the exact characteristics of 5th generation still has not been absolutely clear yet, some of the aimed properties of this generation [Lockheed Martin, 2007] are probably:

- All–aspect stealth property,
- High maneuverability,
- Short field capabilities,
- Advanced avionic features,

– High-performance airframes,

For now, there has been only few type of aircrafts are considered to be named under 5th generation, which are going to be evaluated and taken into consideration while working on the new trainer engine design.

CONSTRAINT AND MISSION ANALYSES

The initial phase of engine design starts with the evaluation of constraint analysis for its aircraft. Performance requirements are obtained with deep research based on potential jet trainer aircraft mission profiles and behaviors.

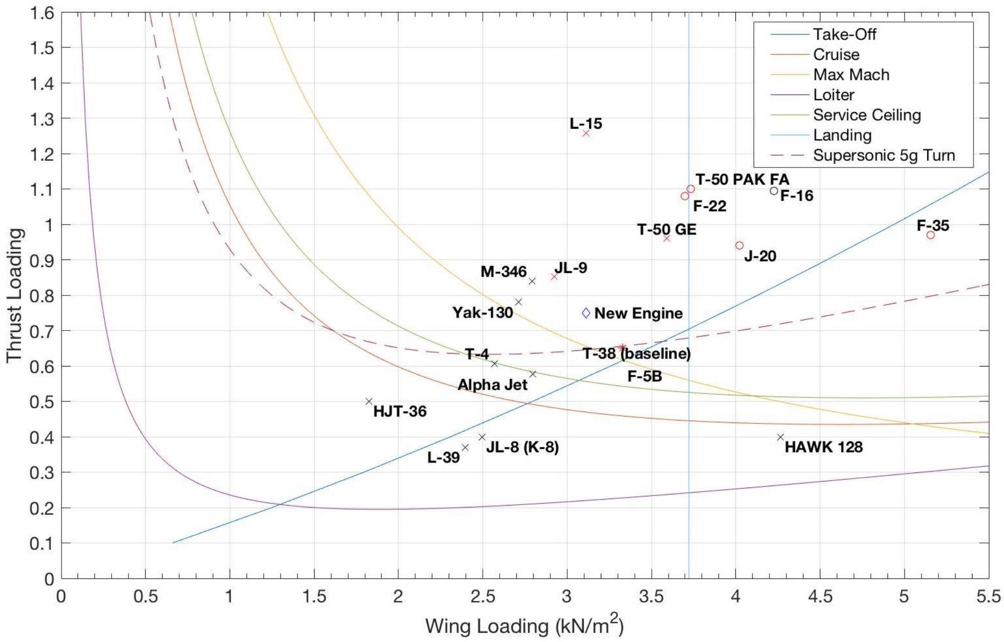

Figure 1: Constraint Diagram - Wing Loading (kN/m^2) vs. Thrust Loading

In the figure 1, (x) points represent trainer aircrafts, (o) points represent fighters and red points represent 5th generation of aircrafts (either developed as 5th generation or modernized to 5th generation). Thanks to baseline engine information from T-38 flight manual [NASA, 2003], distribution of all similar advanced jet trainers and initial evaluation, a design point for the new engine is estimated with targets of engine weight reduction and better fuel efficiency as 0.75 thrust loading and $3.1\ kN/m^2$ wing loading.

A particular new mission profile for new trainer as shown in figure 2 is developed with the help of various examples from other mission profiles of similar aircrafts. Engine requirements are considered together with 5th generation fighter aircraft mission and other examples in the mission profile. Besides, "Combat Simulation" is added to the mission, however it is not specified in details to provide flexibility to the training content. Possible actions under combat simulation might be 1.2 Mach 5g turn, 0.8 Mach 5g 2–turns or acceleration from 0.7 Mach to 1.2 Mach at 4.5 km.

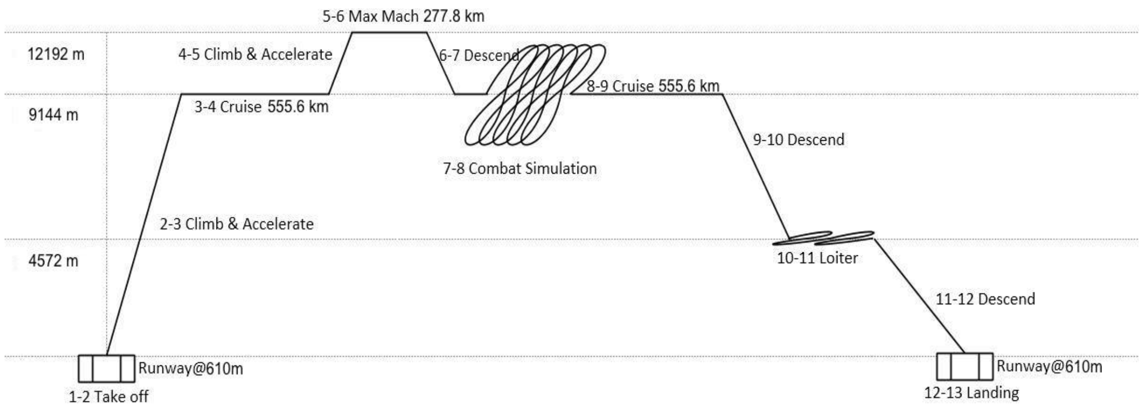

Figure 2: Mission Profile

The maximum range of 2778 km with loiter and almost 3333.6 km without loiter result in a final weight fraction of 0.745, which is very close to 0.74 as shown in figure 3. Therefore, values and calculations seem to be logical for constraint and mission analysis for the desired range.

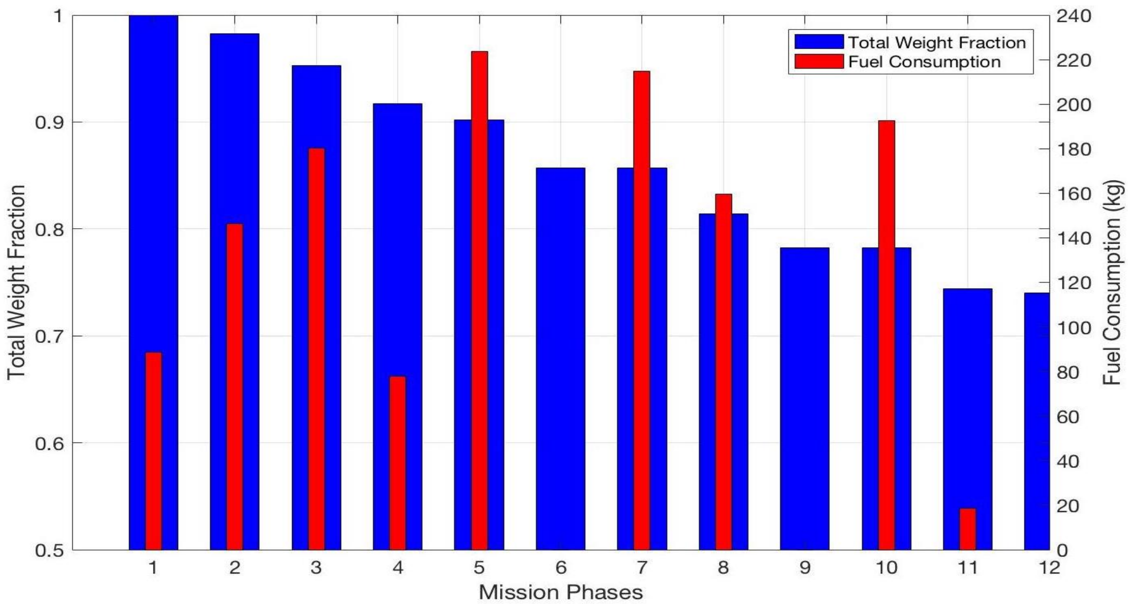

Figure 3: Mission Profile Weight Fraction & Fuel Consumption

PARAMETRIC CYCLE AND PERFORMANCE ANALYSES

Parametric cycle analysis is a dimensionless design to show the connection between major design parameters and how they affect the performance of our engine. Thanks to the variation of each design parameter and their combination, we would be able to perform different working requirements of the engine.

Sea Level Static (SLS) condition is selected for parametric cycle – on design analysis. Other conditions of cruise, supersonic flight and loiter conditions will be evaluated on off-design performance analysis.

Engine Design Variables

In order to determine design parameters, Pareto Principle used which states that the 20% of the main sources / inputs are directly effective on the 80% of the results / outcomes. Therefore, the main design parameters need to be paid most attention. The 6 most important parameters are used in order to make parametric cycle analysis, which are bypass ratio (BPR), operational pressure ratio (OPR), fan/low pressure compressor (LPC) pressure ratio (FPR), high pressure compressor pressure ratio (HPR), turbine inlet temperature (TIT) and afterburner temperature T_{t7}. The historical data and trends together with latest technological capabilities on the on-design cycle analysis are considered from Mattingly [Mattingly et al., 2002] and Farokhi [Farokhi, 2014].

Table 3: Engine Design Variables

Aircraft system parameters	β, P_{TOL}, P_{TOL}, ε_1 ,ε_2
Design limitations	$T_{t4\text{-}max}$, $T_{t7\text{-}max}$
Fuel Heating Value	h_{fuel}
Polytrophic efficiencies	η_{burner}, η_{AB}, η_{mech}, η_{mL}, η_{mH}
Component performances	π_{fd}, π_M
Total pressure losses	π_{intake}, π_{Mmax}, π_{burner}, $\pi_{AfterBurner}$, $\pi_{JetPipe}$, π_{nozzle}
Design Choices	$\dot{m}$, π_f, π_{cL}, π_{cH}, α, T_{t4}, T_{t7}, M_{mix}

Parametric Cycle Analyses

On parametric cycle analysis, design condition is preferred as sea level static condition with $P_{atm} = 1.01325$ MPa and $T_0 = 31.1°$C (SLS + 27F Standart Day).

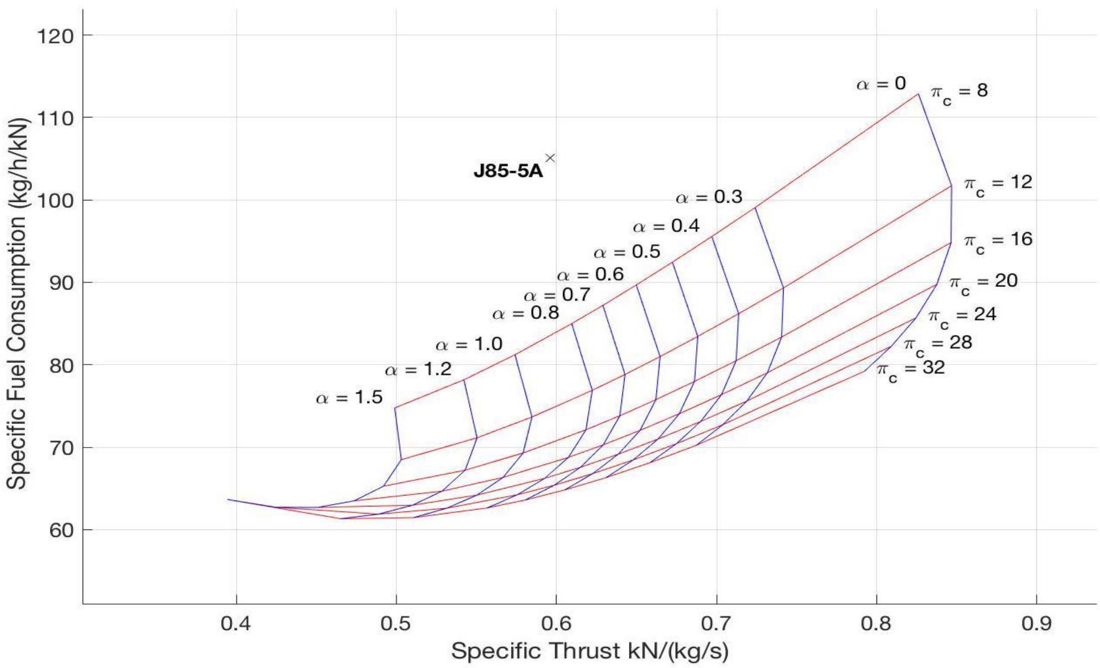

Figure 4: Parametric Cycle Analysis (dry) – BPR vs OPR variation at SLS condition

By-pass ratio above 1.0 provides better fuel consumption efficiencies and difference than lower by-pass ratios. However, on the other hand, increasing by-pass ratio decreases specific thrust value for the engine significantly. Therefore, it is important to select a by-pass ratio that enables the thrust requirements for both on-design and off-design conditions.

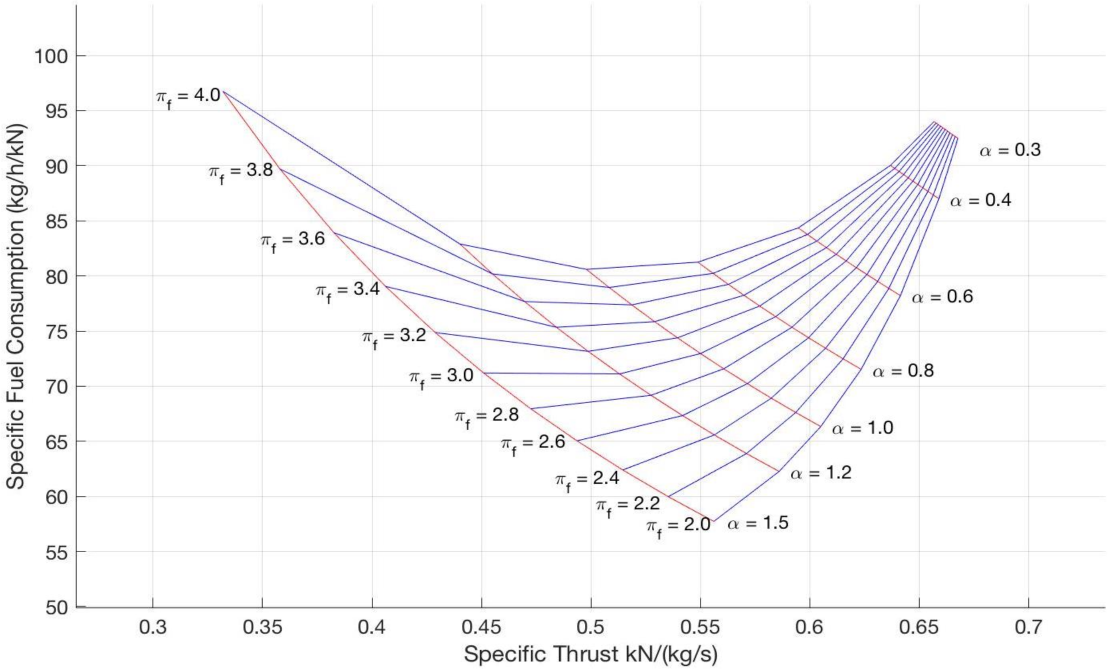

Figure 5: Parametric Cycle Analysis (dry) – FPR vs BPR variation at SLS condition with 16 OPR

Turbine Inlet Temperature (TIT – T_{t4}) has direct relation with SFC and specific thrust values. The baseline engine has 1120 K TIT, however with the consideration of selection new OPR parameter around 16 makes TIT potentially higher than the baseline engine.

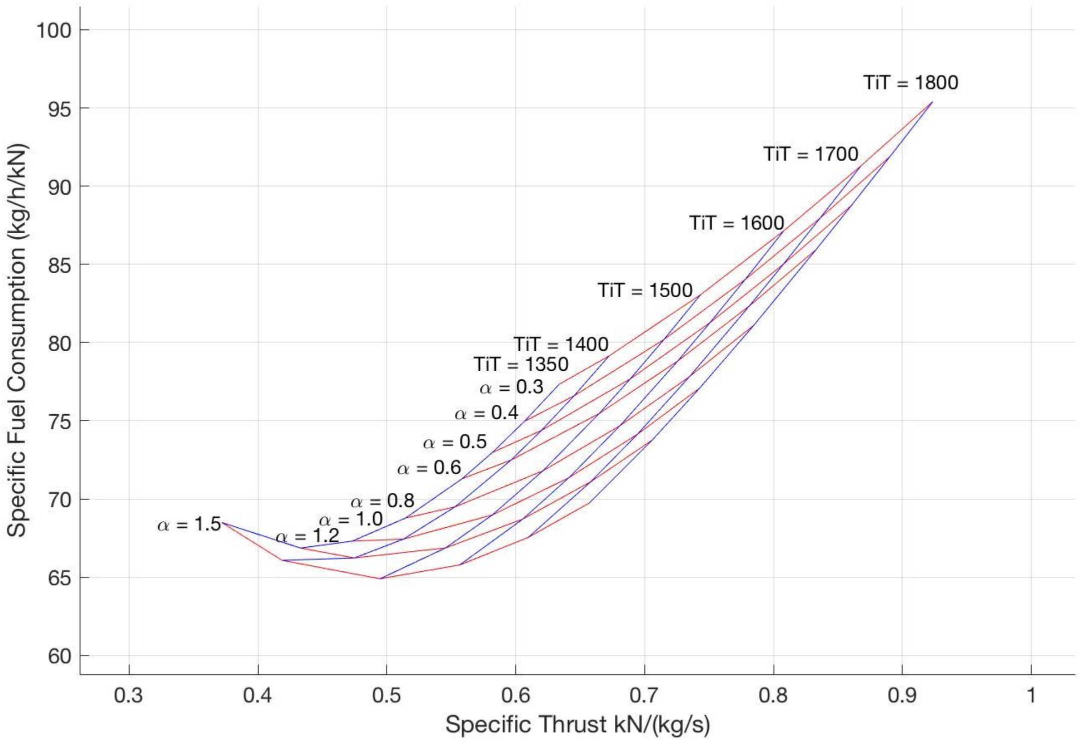

Figure 6: Parametric Cycle Analysis (dry) – BPR vs TIT variation at SLS condition with 16 OPR

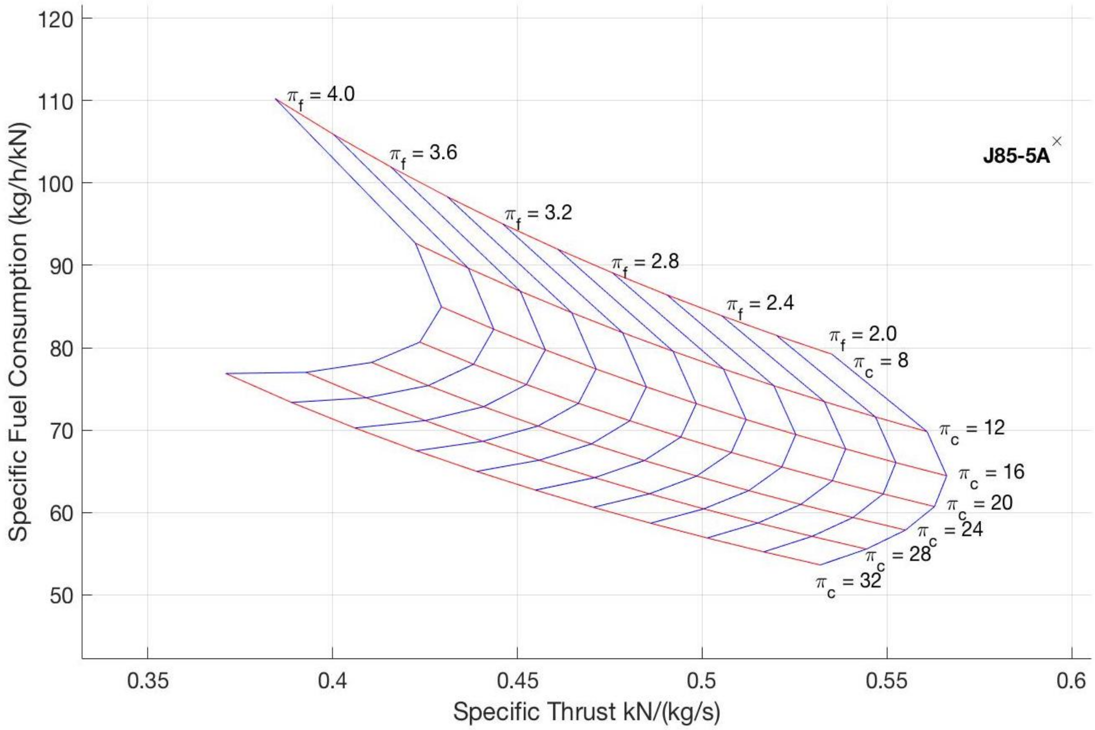

Figure 7: Parametric Cycle Analysis (dry) – FPR vs OPR variation at SLS condition with 1.2 BPR

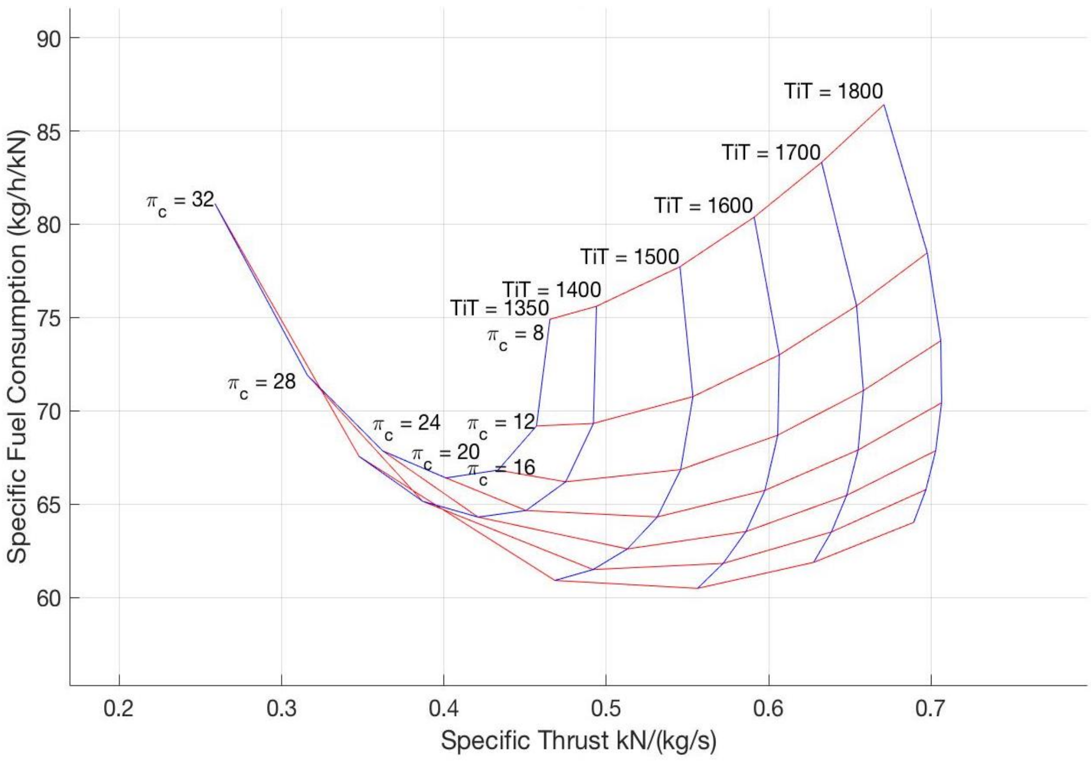

Figure 8: Parametric Cycle Analysis (dry) – OPR vs TIT variation at SLS condition with 1.2 BP1R

The wet conditions of turbofan engine (afterburner is on) are important on the selection of design parameters. Therefore, evaluation of various afterburner values is going to be made. In order to do it, different cases of the design parameter of T_{t7} – maximum afterburner temperature is calculated.

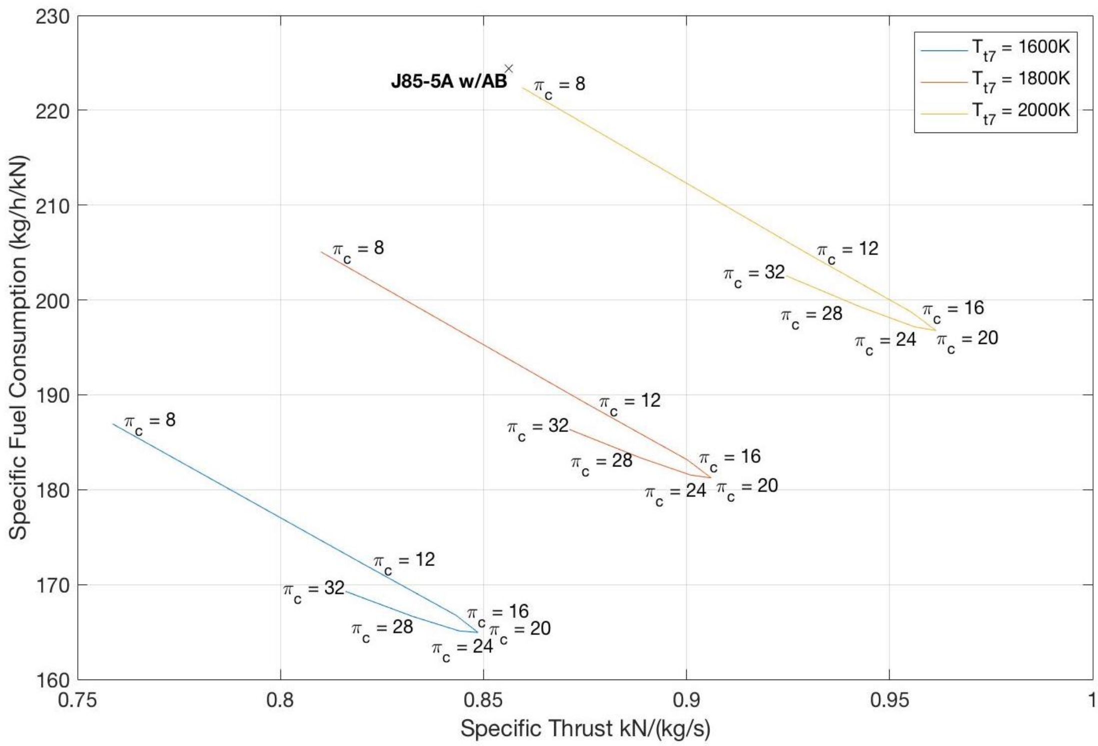

Figure 9: Parametric Cycle Analysis (wet) – OPR vs TIT variation at SLS condition with 1.2 BPR

Thanks to these numerous in-depth parametric analyses, design parameters are chosen as in table 4:

Table 4: Primary Selected Design Values

Primary Selected Design Values			
ByPass Ratio		1.2	
Fan Pressure Ratio		2.3	
Compressor Pressure Ratio		16	
Dry Condition		Wet Condition	
T_{t4} (K)	1500	T_{t7} (K)	1800
Specific Thrust kN/(kg/s)	0.542	Specific Thrust kN/(kg/s)	0.919
SFC (kg/h)/kN	67	SFC (kg/h)/kN	179

Table 5: Parametric Cycle Analysis Summary

Parametric Cycle Analysis Summary (w/AB)			
Station Number	Stagnation Pressure (atm)	Stagnation Temperature (K)	Mass Flow (kg/s)
0	1	303.15	22.68
1	1	303.15	22.68
2	0.96	303.15	22.68
2.5	2.21	396.08	9.90
13	2.21	396.08	12.37
3	15.36	731	9.90
4	14.75	1500	10.44
4.5	5.25	1175.41	10.44
5	2.56	999.43	10.44
16	2.21	396.08	12.37
6A	2.46	647.94	22.81
7	2.33	1800	23.62
9	2.288	1800	23.62

Performance Analyses

The main part of the engine whose operational behavior changes the least is the turbine stage. Both HPT and LPT stages operational pressure and temperature ratios vary so low with the different flight conditions that they can be neglected and assumed as same since both turbines are going to be designed as choking. From the Aircraft Propulsion [Farokhi, 2014] source, in-house program for performance analysis is developed and compared with both AEDsys and GasTurb program results to ensure reliability.

The performance analysis results can be found in table 6.

Table 6: Performance Analyses Results

Performance Analysis Results					
Condition	Loiter	Cruise	Max. Velocity		
	Dry	Dry	Wet		
M_0	0.5	0.85	1.3	1.4	1.5
Mass Flow	34	20	24.30	27.17	30.47
π_f (FPR)	2.305	2.305	2.31	2.31	2.31
π_c (OPR)	16	16	16	16	16
α (BPR)	1.202	1.202	1.21	1.21	1.21
T_{t4} (K)	1341.6	1238.8	1433.2	1490.9	1553.2
T_{t7} (K)	-	-	1800	1800	1800
$\eta_{Thermal}$	37.52%	42.84%	35.43%	37.16%	38.88%
$\eta_{Propulsive}$	44.93%	59.39%	49.45%	51.26%	52.97%
$\eta_{Overall}$	16.85%	25.44%	17.52%	19.05%	20.59%
F_specific (kN/(kg/s))	0.396	0.345	0.912	0.924	0.93
TSFC ((kg/h)/kN)	79.54	82.60	181.51	180.49	178.45
F (kN)	6.10	3.13	10.12	11.39	12.81
$F_{required}$ (kN)	5.47	2.82	6.67		

With the in-house program, it is possible to make further analyses on different flight conditions and create carpet plots to evaluate behaviors of design parameters with each other. These additional in-depth analyses help us to re-evaluate and make necessary updates on the most suitable and efficient design values. The most important condition, cruise is evaluated and fter these additional analyses, initial design choices for new engine seem very good for new engine.

COMPONENTS DESIGN

Inlet

Inlet design is made considering the maximum speed where ramp angles should achieve maximum pressure recovery for that condition. 1.4 Mach speed at 12.19 km altitude corresponds to 22.91 kg/s corrected mass flow and existing nacelle envelope is preferred with less than 45.72 cm fan diameter. New inlet duct is going to be a transition duct to provide variable shape form a rectangular to a circular geometry. Oswatitsch [Goldsmith and Seddon, 1993] introduced a method on similar external compression ramp inlets. In order to reach out the maximum pressure recovery, oblique shocks should have same power, which is used in the inlet ramp angles design phase. Lastly, due to the boundary layer effect, it is suggested to add 4% safety margin into the area Mattingly [Mattingly et al., 2002].

Table 7: Ramp Angles & Inlet Output

External 2 Ramp Compression			
M_1		1.4	
1st Oblique Shock		2nd Oblique Shock	
θ_1	4.367	θ_2	3.759
β_1	51.71	β_2	62.179
M_2	1.24102102	M_3	1.072491669
P_{t1} / P_{t0}	0.9990	P_{t2} / P_{t1}	0.9990
Normal Shock			
M_4	0.9339	P_{t3} / P_{t2}	0.9996
ΔP_t		0.9975	

In order to meet starting requirement of the engine, bellmouth lip is needed. For 0.35 Mach throat number at static condition, 3.81 cm thick bellmouth lip achieves 96.86% pressure recovery. However, the required inlet area is not enough to overcome starting condition barrier. Therefore, 3.05 cm long elliptical inlet lip design is chosen in order to reach out bigger suction strength on the intake face. Since this estimation needs to be experimentally measured and checked, it is fine to make these basic assumptions to reach out the required inlet area of 0.17 m^2.

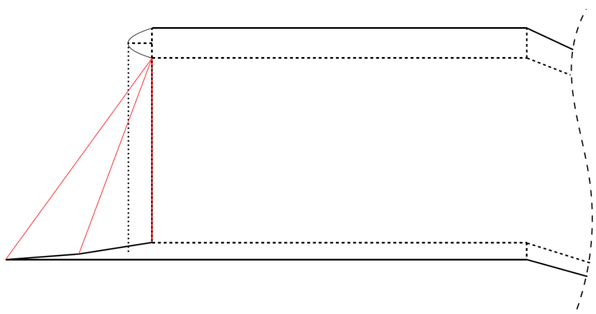

Figure 10: 2D Inlet Geometry with Shock Waves and Bellmouth Lip

After the normal shock, air goes through the transition zone, where the length needs to be as the height of the throat as shown in table 8 [Mattingly et al., 2002]

Table 8: Diffuser Duct

Diffuser Duct	
M_i	0.93
M_e	0.46
A_e / A_i	1.44
L / D	3.5
η_D	0.90
P_{te} / P_{ti}	0.98
Y / D	1.55

The inlet geometrical details are:

- Height: 23.4 cm & Width: 46.8 cm
- Transition duct length: 46.8 cm
- Diffuser length: 1.60 m

Compressor

After reaching certain values on parametric cycle and off-design analyses, design of 2 spool low-bypass turbofan engine will be worked upon. For fan/LPC stage, constant tip line, repeating row, repeating stage design is found appropriate, while for HPC constant mean line, repeating row and repeating stage design is chosen. Both calorically perfect gas and ideal gas properties of air will be used in order to reach the most accurate values. Furthermore, swirl angles assumed as constant and free vortex swirl model has been used.

The most optimum inlet Mach number for new concept is found as 0.58 for the small size of engine in order to be strong and efficient in its all parts. On the other hand, with the increased engine entrance area (higher hub to tip ratio on engine 1st stage compressor), the mass flow is aimed to be increased by $\approx 15\%$ to reach out the 1st estimation of ≈ 22.68 kg/s. Besides, the Mach number before combustion becomes 0.36, which is a good and efficient number, especially for the ultimate technology and newly developed combustion chambers.

Ultimate level to allow diffusion factor value is considered as 0.55. By the evaluation of the aimed design values, solidity ratios 1.1 for fan and 1.5 for HPC are selected. The reason behind the high HPC solidity ratio is the goal of highest fuel consumption for a potential new engine. Because of the significant performance damage of very high solidity ratios, 1.5 is a good combination of intense and successful HPC chapter.

Fan/Low Pressure Compressor (LPC) Design:

On the parametric cycle and off design analyses, low fan pressure ratio design method is decided in order to reach the lowest specific fuel consumption while achieving the required thrust points. The initial design value for fan/LPC, 2.3 pressure ratio is going to be aimed.

Table 9: Fan Design Parameters & Values

Fan Design Parameters	
Number of Stages	2
Mass Flow Rate (kg/s)	22.68
Rotor Angular Speed (rad/s)	~ 1840
Inlet Total Pressure (kPa)	97.29
Inlet Total Temperature (K)	303.15
Entry Angle (degrees)	28.5
Entry Mach	0.58
Diffusion Factor	0.55
Polytropic Efficiency	0.89
Solidity	1.1
Exit Angle for Last Stage (degrees)	28.5
Exit Mach	0.50
Ratio of Specific Heat for Part	1.4
Inlet Diameter (cm)	45.72
Initial Hub to Tip Ratio	0.45
Design Choice	Constant tip

Important design limits of flow coefficient, stage loading and De Haller Criterion are all met with allowable margins. Tip Mach number is around 1.3, which is a common value for military aircraft engines. The tip supersonic velocity would be taken under control with twist angle through the end of fan blades. Moreover, degree of reaction value of both fan stages are around 0.5, which is highly satisfactory for both stages to share the burden of the static temperature rise. By all the calculations, successful diffusion factor is proven.

Corresponding velocity triangles and blade stresses are found as in figure 11 and table 10.

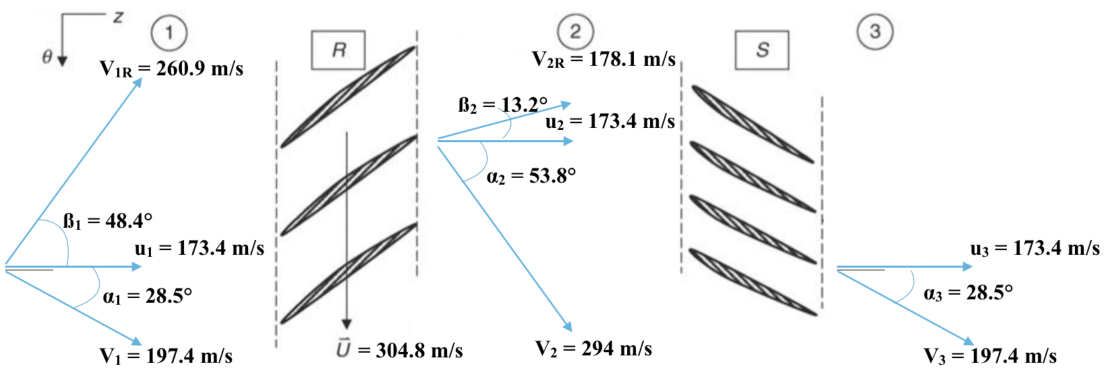

Figure 11: Fan/LPC 1st Stage Velocity Triangles (mean)

Table 10: Fan/LPC Blade Stress Calculations

Fan Blade Stress Calculations			
Stage 1		Stage 2	
W_{r1} (cm)	5.13	W_{r3} (cm)	3.33
W_{s2} (cm)	3.84	W_{s4} (cm)	3.33
h_1 (cm)	12.57	h_3 (cm)	8.08
h_2 (cm)	10.67	h_4 (cm)	6.99
A (m^2)	0.13	A (m^2)	0.10
σ_{c1} (MPa)	279.15	σ_{c2} (MPa)	281.12
AN^2 (10^{10})	5.95	AN^2 (10^{10})	5.98

High Pressure Compressor (HPC) Design: Most of the fan/LPC assumptions are also valid for HPC design. The major difference is on the design type, which constant mean line method is used for this part as the reason of lower relative mean radius and easier repeating stages design. Besides, due to the separation of bypass and main core of the engine, this method is easier to produce and establish for new engine model without extra length or weight requirements.

Table 11: HPC Design Parameters & Values

High Pressure Compressor Design Parameters	
Number of Stages	6
Mass Flow Rate (kg/s)	10.43
Rotor Angular Speed (rad/s)	2700
Inlet Total Pressure (kPa)	221.94
Inlet Total Temperature (K)	392
Entry Angle (degrees)	26.8
Entry Mach	0.50
Diffusion Factor	0.55
Polytrophic Efficiency	0.90
Solidity	1.5
Exit Angle for Last Stage (degrees)	26.8
Exit Mach	0.36
Ratio of Specific Heat for Part	1.39
Inlet Mean Radius (cm)	13.72
Initial Hub to Tip Ratio	0.75

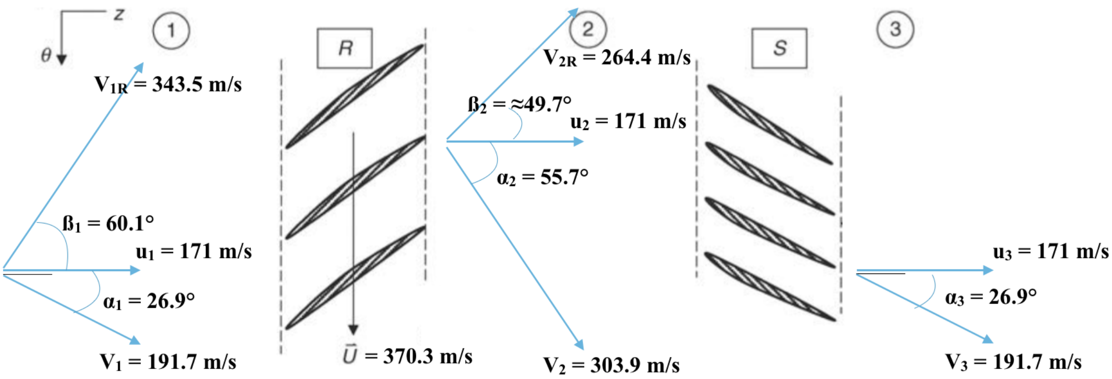

Figure 12: HPC 1st Stage Velocity Triangles (mean)

Table 12: HPC Blade Stress Calculations

HPC Blade Stress Calculations					
Stage 3		**Stage 4**		**Stage 5**	
W_{r5} (cm)	1.42	W_{r7} (cm)	1.04	W_{r9} (cm)	0.81
W_{s6} (cm)	1.19	W_{s8} (cm)	0.91	W_{s10} (cm)	0.71
h_5 (cm)	4.32	h_7 (cm)	3.07	h_9 (cm)	2.36
h_6 (cm)	3.56	h_8 (cm)	2.67	h_{10} (cm)	2.06
A (m^2)	0.04	A (m^2)	0.03	A (m^2)	0.02
σ_c (MPa)	146.16	σ_c (MPa)	139.94	σ_c (MPa)	138.3
AN^2 (10^{10})	1.85	AN^2 (10^{10})	1.77	AN^2 (10^{10})	1.75
Stage 6		**Stage 7**		**Stage 8**	
W_{r11} (cm)	0.64	W_{r13} (cm)	0.51	W_{r15} (cm)	0.43
W_{s12} (cm)	0.56	W_{s14} (cm)	0.46	W_{s16} (cm)	0.38
h_{11} (cm)	1.85	h_{13} (cm)	1.50	h_{15} (cm)	1.24
h_{12} (cm)	1.65	h_{14} (cm)	1.35	h_{17} (cm)	1.12
A (m^2)	0.02	A (m^2)	0.01	A (m^2)	0.01
σ_c (MPa)	136.79	σ_c (MPa)	135.38	σ_c (MPa)	134.05
AN^2 (10^{10})	1.73	AN^2 (10^{10})	1.71	AN^2 (10^{10})	1.70

Since both stages need materials that are able to resist high stresses, Titanium Alloy (Ti-6Al-4V) for fan/LPC and Greek Ascoloy for HPC seems suitable. However, for weight and cost reduction purposes, a potential mixtures with other materials have also potential for this new compressor stage.

Combustor

Because of maximum dynamic pressure effect, sea level static condition is considered for the main combustor. Annular type provides weight advantages and higher pressure recovery, therefore preferred. Flat wall geometry with 2 splitters as diffuser system is designed. Splitters enable shorter and more efficient operations by slowing down the incoming air coming from the compressor with the value of 0.35 Mach. Corresponding length of the diffuser is 4.93 cm with 4.88 cm axial length. With the adequate mix, burner total pressure loss results as 69.22 kPa. This is approximately 80% of the allowable value, 84.74 kPa and therefore acceptable.

Table 13: Main Burner Stations & Dimensions

Stations Dimensions	Station 3.1	Station Burner	Station 4
R_{outer} (cm)	14.18	15.93	16.00
R_{inner} (cm)	13.25	12.72	14.48
R_{mean} (cm)	13.72	14.33	15.24
H (cm)	0.92	3.21	1.52

Table 14: Combustor Air Partitions

Air Partitions	Total	Primary Zone	Secondary Zone	Transpiration Cooling	Dilution Zone
Air Flow (kg/s)	10.31	4.51	1.93	1.65	2.22
Mass Fraction	1.000	0.438	0.188	0.160	0.215

Swirler blade geometry with 0.64 drag coefficient and 40 blade angle is chosen. Corresponding swirl number is found as 0.76, which is a good value between 0.60 – 1.00. Further swirler details, combustor layout and properties are shown in figure 13, tables 15 and 16.

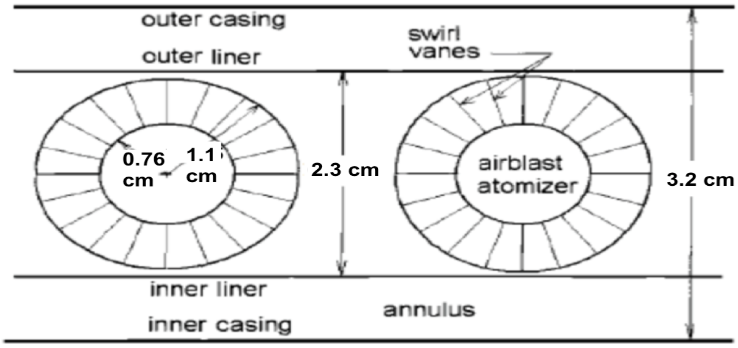

Figure 13: Swirler Design & Layout

Table 15: Main Burner Zones Geometry

Zones Geometry			
$N_{primary}$	28	$L_{primary}$ (cm)	1.67
$N_{secondary}$	260	$L_{secondary}$ (cm)	4.42
$N_{dilution}$	168	$L_{dilution}$ (cm)	3.31

Table 16: Main Burner Geometry

Burner Geometry	
Length (cm)	9.41
Diameter (cm)	3.21
Total Volume (m^3)	2.72×10^{-3}
Combustion Zone (m^3)	2.1×10^{-3}

Turbine

Primary goal turbine design is to design the turbine stage models according to the rest of the engine in order to meet the parametric on-design requirements, and also off-design operation conditions. Single stage high pressure turbine (HPT) and low pressure turbine (LPT) design is preferred due to increased pressure ratio of new engine. Besides, for the HPT stage, cooling with a very low percentage of air due to contribution of the component life and durability of material. Cooling helps engine to have an extra control on the turbine inlet temperature, which is useful for various flight conditions and extreme throttle ratio scenarios of 5th generation aircrafts, such as high-g maneuvers and accelerations.

High Pressure Turbine (HPT) Design:

Table 17: HPT Design Parameters (0 M & Sea Level)

High Pressure Turbine Design Parameters					
τ_{tH}	0.80	$P_{t4.1}$ (kPa)	1510.09	γ_t	1.33
π_{tH}	0.358	$T_{t4.1\text{-}max}$ (K)	1600	$g_c * c_p$ ($m^2/(s^2*K)$)	1119.44
N (rpm)	25783.10	$\dot{m}$ (kg/s)	10.52	R (m*kN/(kg*K))	0.306

For the design parameters of turbine, M_1, M_2 and M_{3R} are used to make rest of the calculations. Besides, in order to shape the geometry of turbine, mean radius is selected as 0.15m. Constant heat capacity ratio value of calorically perfect gas, ideal gas property of air and polytrophic efficiency values are used into calculations. As last, u_3/u_2 is used as 0.9 to ensure the target of relative Mach number. Design parameters and chosen values are; turbine entrance Mach as 0.3, HPT vane exit Mach as 1.15 to ensure the choking flow, HPT rotor Exit Mach as 0.8 and HPT vane exit angle as 70°. M_2 is taken as supersonic to make sure flow is choked and M_{3R} is taken subsonic.

Corresponding HPT velocity triangles, blade stresses and results are found as in figure 14, tables 18 and 19 respectively.

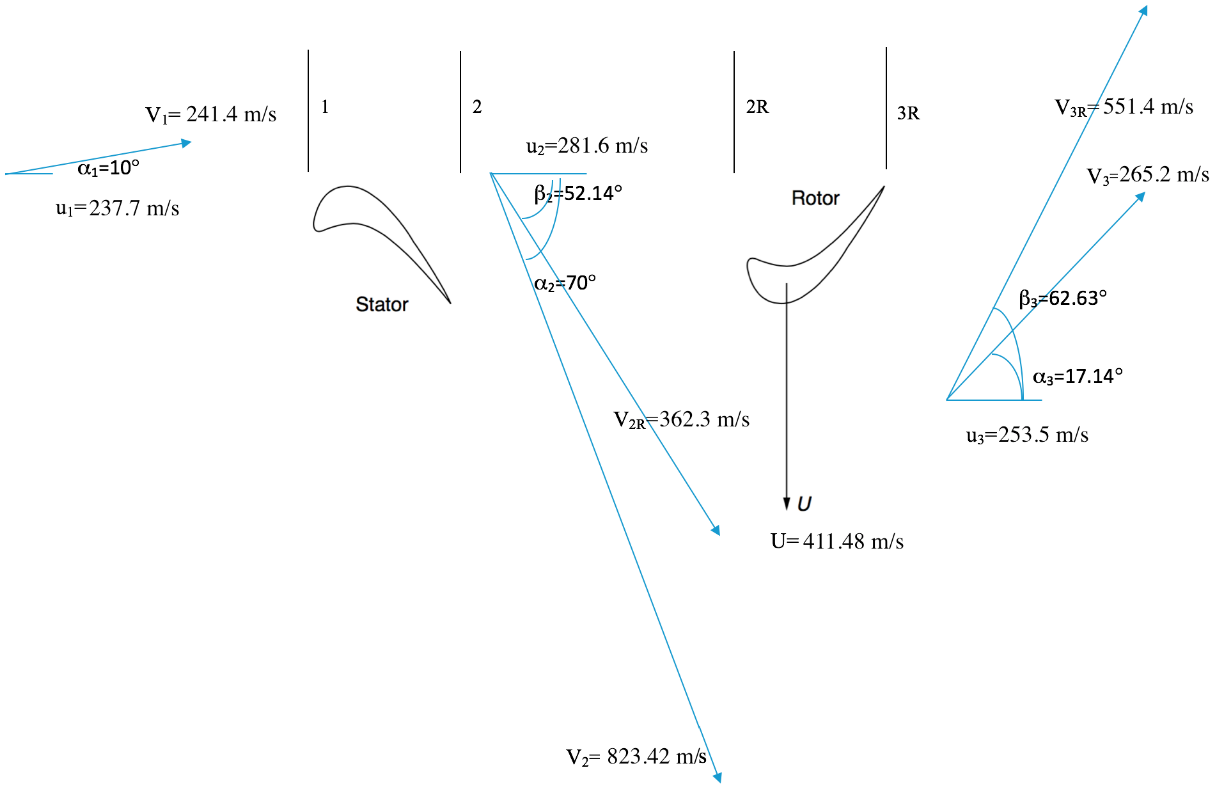

Figure 14: HPT Stage Velocity Triangles (mean)

Table 18: HPT Blade Stress Calculations

1st Stage Turbine (HPT) Blade Stresses			
Blade Widths Vane		**Blade Widths Rotor**	
W_{vane} (cm)	1.77	W_{rotor} (cm)	2.87
h_1 (cm)	1.68	h_{2R} (cm)	2.36
h_2 (cm)	2.36	h_{3R} (cm)	3.42
Stress Calculations			
W_{dr} / W_{vane}	0.56	W_{dr} / W_{rotor}	0.56
$W_{dr\text{-}rim}$ (cm)	0.99	$W_{dr\text{-}rim}$ (cm)	1.60
h_r / r_r	0.05	h_r / r_r	0.05
r_r (cm)	13.72	r_r (cm)	12.88
ρ_1 (kg/m³)	2.93	ρ_2 (kg/m³)	1.762
$\lambda_{Taper\ Ratio}$	0.70	$\lambda_{Taper\ Ratio}$	0.70
A_1 (cm²)	226.02	A_2 (cm²)	327.92
σ_c (MPa)	301.93	σ_c (MPa)	263.45
A_{ave} (cm²)		276.97	
$\sigma_{c\text{-}ave}$ (MPa)		282.69	

Table 19: HPT Results

Stage Loading	Flow Coefficient	Isentropic Efficiency	Aspect Ratio		Solidity		Blade Numbers	
			Vane	Rotor	Vane	Rotor	Vane	Rotor
1.684	0.578	0.902	1.000	1.000	0.969	1.353	55	55
					Preferred Design Choice			
					1.2	**2**	**68**	**80**

Cooled-turbine stage efficiency is 0.902. When compare this value with Smith Chart for turbine stage efficiencies, it seems consistent.

Low Pressure Turbine (LPT) Design:

Table 20: LPT Design Parameters (0 M & Sea Level)

Low Pressure Turbine Design Parameters					
τ_{tL}	0.85	$P_{t4.5}$ kPa	540.62	γ_t	1.33
π_{tL}	0.49	$T_{t4.5}$ (K)	1260.06	$g_c * c_p$ (m²/(s²*K))	1066
N (rpm)	17561.92	$\dot{m}$ (kg/s)	10.85	R (m*kN/(kg*K))	0.294

Design parameters and chosen values are; LPT entrance Mach as 0.38, LPT vane exit Mach as 1.10 to ensure the choking flow, LPT rotor Exit Mach as 0.78 and LPT vane exit angle as 60°. u_5/u_4 is again used as 0.9 to ensure the target of relative Mach number.

Corresponding HPT velocity triangles, blade stresses and results are found as in figure 15, tables 21 and 22 respectively.

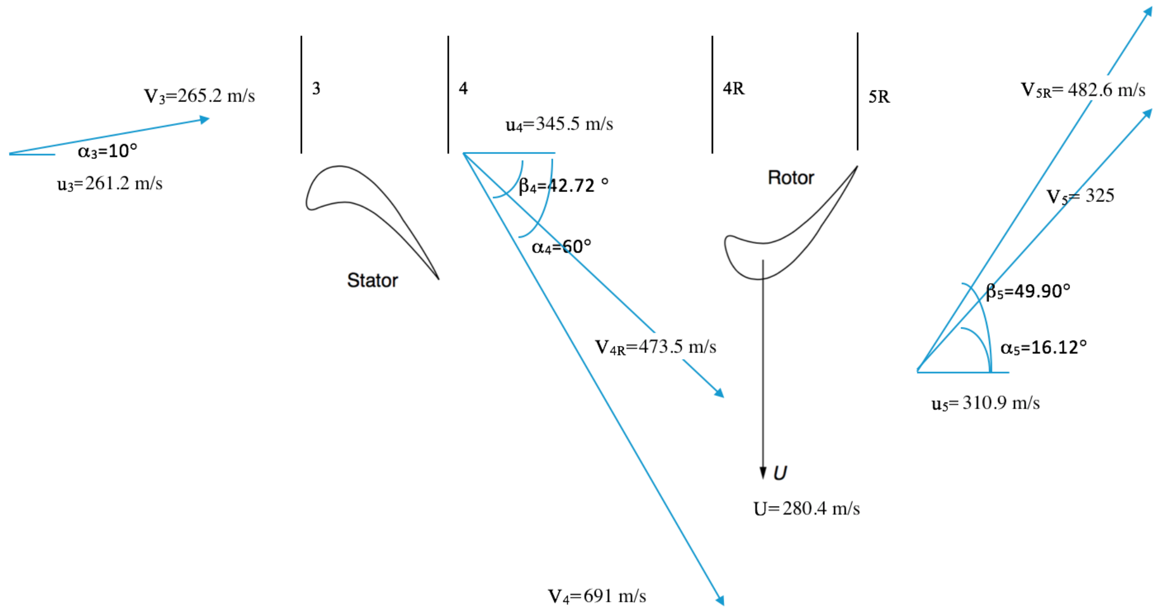

Figure 15: LPT Stage Velocity Triangles (mean)

Table 21: LPT Blade Stress Calculations

2nd Stage Turbine (LPT) Blade Stresses			
Blade Widths Vane		**Blade Widths Rotor**	
W_{vane} (cm)	3.30	W_{rotor} (cm)	4.33
h_3 (cm)	3.28	h_{4R} (cm)	3.91
h_4 (cm	3.91	h_{5R} (cm)	4.80
Stress Calculations			
W_{dr} / W_{vane}	0.5600	W_{dr} / W_{rotor}	0.5600
$W_{dr\text{-}rim}$ (cm)	1.85	$W_{dr\text{-}rim}$ (cm)	2.42
h_r / r_r	0.05	h_r / r_r	0.05
r_r (cm)	12.95	r_r (cm)	12.23
ρ_3 (kg/m³)	1.36	ρ_4 (kg/m³)	0.75
$\lambda_{Taper\ Ratio}$	0.70	$\lambda_{Taper\ Ratio}$	0.70
A_3 (cm²)	314.59	A_4 (cm²)	459.51
σ_c (MPa)	195.00	σ_c (MPa)	159.51
A_{ave} (cm²)		387.03	
$\sigma_{c\text{-}ave}$ (MPa)		177.26	

Table 22: LPT Results

Stage Loading	Flow Coefficient	Isentropic Efficiency	Aspect Ratio		Solidity		Blade Numbers	
			Vane	Rotor	Vane	Rotor	Vane	Rotor
1.822	0.638	0.917	1.000	1.000	0.997	1.753	30	44
					Preferred Design Choice			
					1.2	**2**	**36**	**50**

Stage loading, flow coefficient and isentropic efficiency are checked to ensure consistency between vane and rotor boundaries. Un-cooled turbine stage efficiency is 0.917.

To conclude turbine section, ultimate technology CMC (ceramic matrix composite) is the well suited material for turbine blades. For both of the turbine stages, C/SiC composite is selected for the vane and rotor blades due to their higher tensile strength, higher operational temperature limits, strong resistance for oxidization and stability to corrosion.

Mixer & Afterburner

With the same engine diameter and mixer-diffuser type choice, mixer component is designed. The most important criteria for this section is to make sure velocities coming from turbine and bypass duct are matching each others value, which otherwise would cause structural damages inside the engine.

Table 23: Flow Areas before After-Burner Section

Dimensions	Station 5	Station 6	Station 13	Station 16	Station 6A	Station 7
r_{outer} (cm)	17.64	18.44	22.86	22.10	22.86	22.86
r_{mean} (cm)	15.24	13.02	21.34	20.27	16.00	11.43
r_{inner} (cm)	12.84	19.28	19.81	18.44	9.14	0.000
A (m²)	0.046	0.089	0.041	0.047	0.138	0.164
H (cm)	4.80	10.85	3.05	3.66	13.72	22.86

On the 7th stage, mixed stream velocity is calculated as 134.11m/s, which is 0.257 Mach at ≈ 650K.

Mixer optimum area is calculated by Mattingly [Mattingly et al., 2002] equations and a desirable diffuser efficiency value obtained as 96.4%.

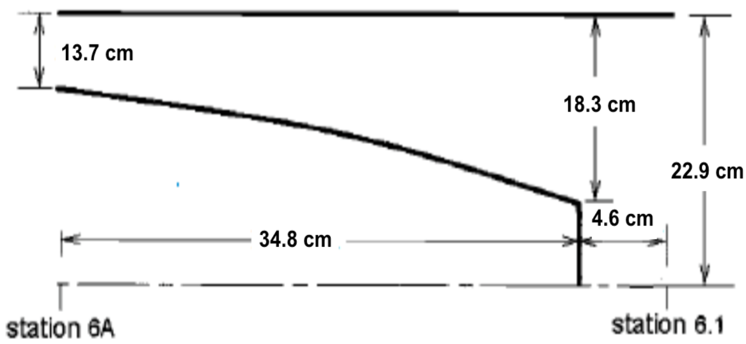

Figure 16: Mixer & Diffuser Layout

$2 = 30^{\circ}$ Vee-Gutter angle is chosen for flame holders. Moreover, W/H value of 0.4 corresponds to 0.314 D/H is selected in order to minimize pressure loss on the afterburner section.

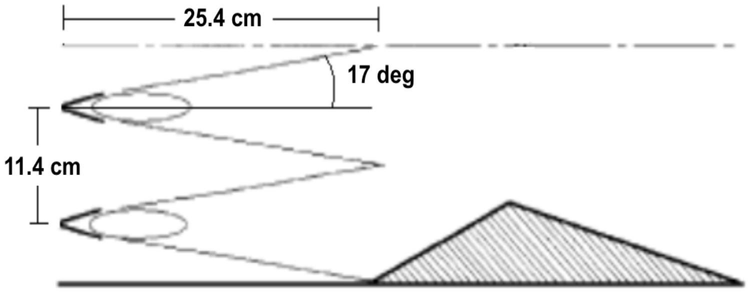

Figure 17: Flameholders Layout

Nozzle

One of the key components that has direct significant effect on specific fuel consumption and thrust is nozzle. Nozzle is responsible from increasing the velocity of the exhaust gas to enhance kinetic energy for obtaining a higher thrust value.

Taking into consideration of efficient expansion of gasses to ambient pressure, low installation drag, noise restrictions and low cooling requirements with light-weight system; an appropriate convergent-divergent noise-attenuating nozzle which enables efficient supercruise and current noise restrictions at take-offis designed.

Afterburner operations forces a variable nozzle area design. Moreover, high maneuverability of 5th generation fighter aircrafts is a result of both variable nozzle area and thrust vectoring. In order to simulate similar behaviors in the training simulations, these properties are taken into consideration. Furthermore, circular nozzle throat type is preferred because of its higher pressure recovery compared to the rectangular nozzle throat [Mattingly, 2002].

2 major flight conditions of the aircraft determines the variable nozzle area; minimum mass flow passing through nozzle on cruise condition (dry) and maximum amount of mass flow passing through nozzle on maximum speed condition (full wet). Because of aimed increased maximum speed, 1.4 Mach is considered.

Table 24: Nozzle Design Values

Nozzle Design Input	Flight Condition	
	Cruise at 10.67 km	Max Mach at 12.19 km
Mass Flow Rate (kg/s)	9.17	12.90
Pressure Loss	0.988	0.988
Throat Mach Number	1.00	1.00
Flight Mach Number	0.85	1.4
T_{t8} (K)	539.8	1600
P_{t9} / P_0	3.83	7.20
Exit Mach Number (real)	1.53	1.96
A_9 / A_8	1.20	1.71
Max Discharge Coefficient	0.94	0.98

Table 25: Nozzle Design Results

Nozzle Design Output	Flight Condition	
	Cruise at 10.67 km	Max Mach on 12.19 km
Exit Mach Number (ideal)	1.54	1.97
Exit Mach Number (real)	1.53	1.96
Velocity Coefficient	0.995	0.9975
Primary Half Angle (degrees)	30.7	17.01
Secondary Half Angle (degrees)	3.4	14.38
Throat Radius (cm)	13.56	18.06
Exit Radius (cm)	14.86	23.62
Primary Nozzle Length (cm)	15.67	
Secondary Nozzle Length (cm)	21.69	
Total Nozzle Length (cm)	37.36	

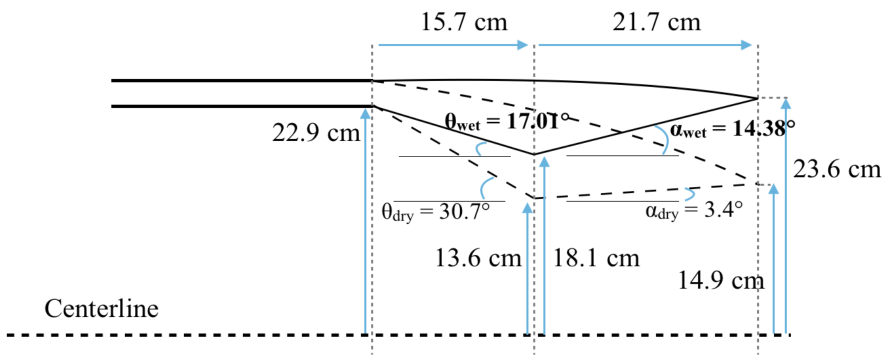

Figure 18: Convergent-Divergent Nozzle Geometry

ENGINE WEIGHT ESTIMATION

Engine Weight Estimation and Analyses

For engine weight estimation, WATE++ program developed by NASA in collaboration with Boeing [Greitzer and Slater, 2002] is used. The simplified version of this method uses OPR, BPR and mass flow parameters in order to estimate approximate engine weight.

$$W_{Engine} = \alpha \times \left(\frac{\dot{m}_{core}}{100}\right)^b \times \left(\frac{OPR}{40}\right)^c$$

For the engines with current technology (late 1990?s through mid-2000s):

- a $= (-6.590 \times 10^{-1})BPR^2 + (2.928 \times 10^2)BPR + 1915$
- b $= (6.784 \times 10^{-5})BPR^2 - (6.488 \times 10^{-3})BPR + 1.061$
- c $= (-1.969 \times 10^{-3})BPR + 0.0711$

For the engines with advanced materials (including carbon composites, CMC, MMC, and TiAl) :

- a $= (-6.204 \times 10^{-1})BPR^2 + (2.373 \times 10^2)BPR + 1702$
- b $= (5.845 \times 10^{-5})BPR^2 - (5.866 \times 10^{-3})BPR + 1.045$
- c $= (-1.918 \times 10{-}3)BPR + 0.0677$

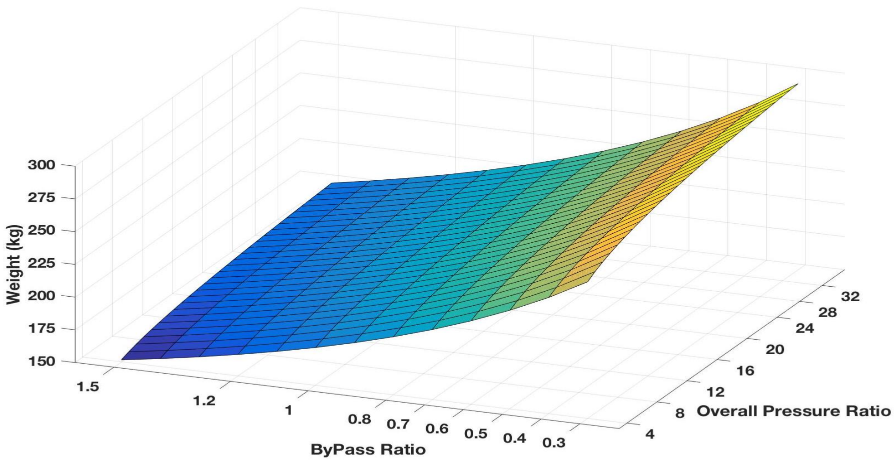

Figure 19: Engine Weight Estimation Graph (Mass Flow 22.68 kg/s)

The unit of these equations is based on BI system, which is converted into SI during the calculations. The accuracy of the equation system is checked and compared with industrial engines to make sure found engine weight is reliable.

CONCLUSIONS

New conceptual design and baseline engine comparison is shown in table 26.

Table 26: J85-5A & New Engine Comparison Summary

	J85-GE-5A		New Engine	
Properties	DRY	WET	DRY	WET
Thrust (kN)	11.92	17.13	12.23	20.46
TSFC (kg/h/kN)	105	224	67	179
Airflow (kg/s)	20.00		22.68	
OPR	6.7		16	
ByPass Ratio	-		1.2	
Compressor Stages	9		2F, 0L, 6H	
Turbine Stages	2		1H, 1L	
Diameter (cm)	55.88		50.80 (45.72 by Fan)	
Length (m)	2.75		2.03	
Weight (kg)	264.90		192.78	

A summary of selected materials for each component is listed in table 27:

Table 27: New Engine Components vs. Material Summary

Components	Material
Fan / LPC	Ti-6Al-4V
HPC	Greek Ascoloy
Burner	SiC/SiC Composite (CMC)
HPT	C/SiC Composite (CMC)
LPT	C/SiC Composite (CMC)
Nozzle	Ti-MMC (Metal Matrix Composite)

2D and 3D technical drawings of the design is shown in figures 20 and 21.

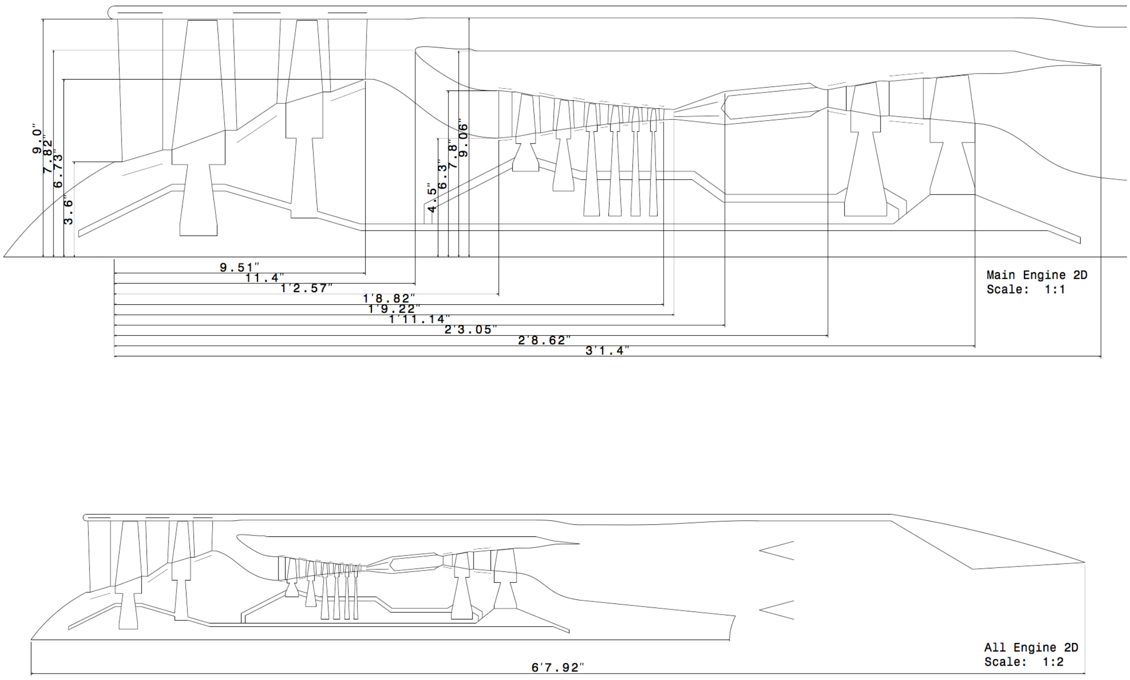

Figure 20: 2D Technical Drawing

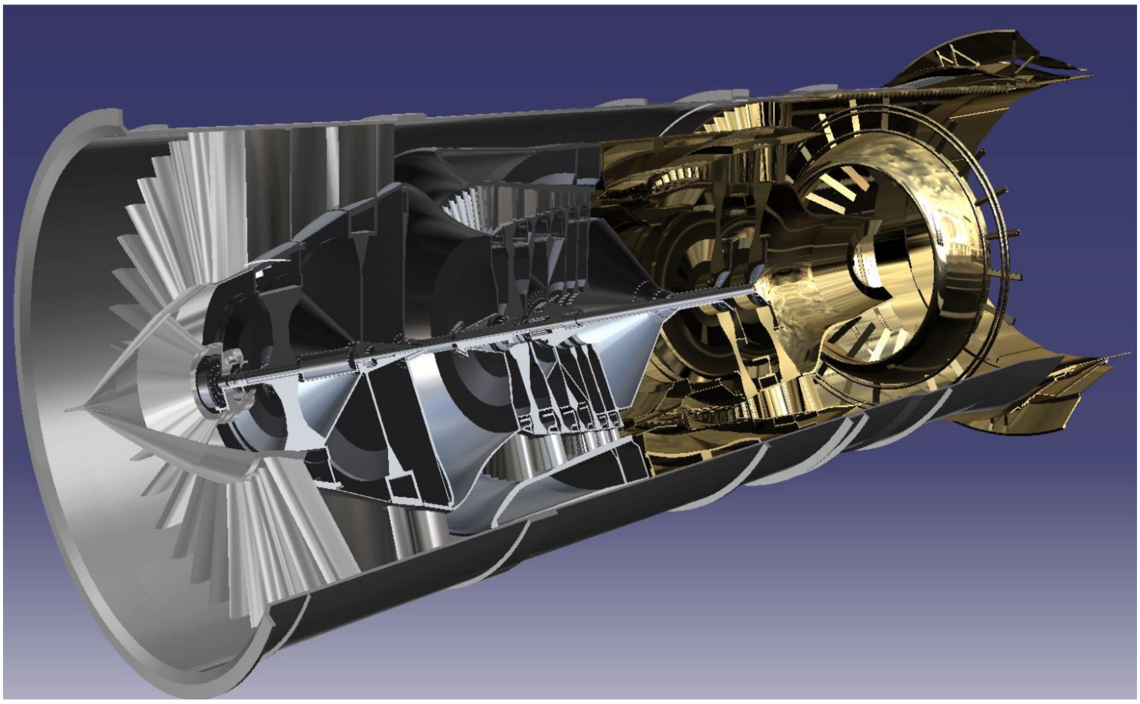

Figure 21: 3D Technical Drawing

New conceptual design achieves better performance and efficiencies for new version of T-38 jet trainer.

FUTURE RECOMMENDATIONS

Because of the small size of the engine, further analyses are recommended to ensure the reliability of this concept. Especially boundary layer and CFD analyses of the compressor and turbine components would be very useful. Since this conceptual design is originally prepared for AIAA design competition for the subject of 2016, these analyses are not made for this work.

ACKNOWLEDGEMENTS

The authors and ITU BeEngine Team acknowledge the support and sponsorship of GE Aviation Turkey, Turkish Airlines and Istanbul Technical University for the final stage of AIAA Team Engine Design Competition 2016 at Joint Propulsion Conference.

The original and more detailed study of this subject can be found on AIAA website section 2015–2016 Design Competition Winning Reports under Undergraduate Team Engine Design as 2nd with the title of "ITU BeEngine for a Next Generation Trainer".

NOMENCLATURE

BPR: Bypass Ratio – α
CFD: Computational Fluid Dynamics
CMC: Ceramic Matrix Composite
η: Polytropic Efficiency
FPR: Fan Pressure Ratio
h: height
HPC: High pressure compressor
HPT: High Pressure Turbine
LPC: Low Pressure Compressor
LPT: Low Pressure Turbine
$\dot{m}$: Mass Flowrate
M: Mach Number
MMC: Metal Matrix Composite
NASA: National Aeronautics and Space Administration
OPR: Operational (Overall) Pressure Ratio
π: Pressure Ratio
P_x: Static Pressure at station x
P_{tx}: Total Pressure at station x
r: radius
σ: Stress
SFC: Specific Fuel Consumption
SiC: Silicon Carbide
SLS: Sea Level Static
τ: Temperature Ratio
T_x: Static Temperature at station x
T_{tx}: Total Temperature at station x
T_{t7}: After-Burner Temperature
TSFC: Thrust Specific Fuel Consumption
TIT: TSFC: Thrust Specific Fuel Consumption

References

Farokhi, S. (2014) *Aircraft Propulsion*, John Wiley & Sons, 2nd Ed.

Greitzer E.M. and Slater H.N. (2010) *Design Methodologies for Aerodynamics, Structures, Weight, and Thermodynamic Cycles – Final Report*, MIT - Aurora Flight Sciences and Pratt & Whitney Team.

Goldsmith, E.L. and Seddon, J. (1993) *Practical Intake Aerodynamic Design*, AIAA.

Heiser, W.H., Mattingly, J.D. and Pratt, D.T. (2002) *Aircraft Engine Design*, AIAA, 2nd Ed.

Lockheed Martin (2007) *F-35 Defining the Future*.

NASA (2003) *T-38 Flight Manual*.